# Transition from Beam-Target to Thermonuclear Fusion in High-Current Deuterium Z-Pinch Simulations

Dustin T. Offermann, Dale R. Welch, Dave V. Rose, Carsten Thoma, Robert E. Clark, Chris B. Mostrom, Andrea E. W. Schmidt, and Anthony J. Link

Phys. Rev. Lett. **116**, 195001 — Published 9 May 2016

DOI: 10.1103/PhysRevLett.116.195001

# The Transition from Beam-Target to Thermonuclear Fusion in High-Current, $D_2$ Z-Pinch Simulations

Dustin T. Offermann,* Dale R. Welch, Dave V. Rose, Carsten Thoma, Robert E. Clark, and Chris B. Mostrom
*Voss Scientific, LLC, Albuquerque, New Mexico 87108, USA*

Andrea E.W. Schmidt and Anthony J. Link
*Lawrence Livermore National Laboratory, Livermore, California 94551, USA*

Fusion yields from dense, Z-pinch plasmas are known to scale with the drive current, which is favorable for many potential applications. Decades of experimental studies, however, show an unexplained drop in yield for currents above a few MA. In this work, simulations of DD Z-Pinch plasmas have been performed in 1-D and 2-D for a constant pinch time and initial radius using the code LSP, and observations of a shift in scaling are presented. The results show that yields below 3 MA are enhanced relative to pure thermonuclear scaling by beam-like particles accelerated in the Rayleigh-Taylor induced electric fields, while yields above 3 MA are reduced because of energy lost by the instability and the inability of the beam-like ions to enter the pinch region.

PACS numbers: 52.58.Lq,52.65.Rr

Neutron yields in dense Z-pinch experiments and in numerical simulations are generally observed as scaling with the current to the fourth power [1–3]. A deviation from a single $I^4$ scaling exists for currents around a few mega-amps [4]. The constant of proportionality is nearly two orders of magnitude greater for currents below 1-3 MA than it is for currents above that. The drop stands as a barrier to potential applications such as a compact neutron source for imaging diagnostics, radiation therapy, isotope production, etc. and as a source of economical fusion energy [5–8]. The exact cause for the deviation has eluded researchers for nearly 50 years [4]. One proposed explanation is that the introduction of high-Z impurities originating from the erosion of electrodes at high currents, such as in dense plasma focus (DPF) devices, could result in quenching the fusion reactions [9, 10]. Two mechanisms exist which contribute to the total yield, beam-target and thermonuclear fusion. Both mechanisms are shown to scale as $I^4$ in analytic models [2, 3], given a constant pinch time with a constant initial radius. Another possibility for the shift is that a transition from beam-target dominated fusion to thermonuclear dominated fusion exists. For 2 MA, beam-target fusion has been identified as the dominant mechanism in gas puff experiments [11]. In 15 MA experiments, the dominant mechanism for fusion has been shown to be thermonuclear [12]. Estimations of the fractional yield by thermonuclear fusion from fully kinetic simulations of gas puff pinches by Welch *et al.*[13] support this hypothesis.

In this work, a computational investigation of fundamental plasma physics effects which contribute to the observed change in scaling is presented. One and two dimensional, cylindrical simulations of a gas puff Z-pinch were performed using the hybrid, particle-in-cell (PIC) code, LSP [14, 15] for currents ranging from 1 to 15 MA. Neutron yields from simulations with and without significant Rayleigh-Taylor (RT) features are presented. The current scan was performed with a constant pinch velocity by keeping $I^2/\rho_0$ = constant for a constant initial radius.

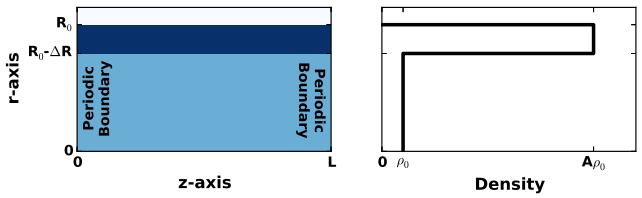


FIG. 1. (color online). The initial density profile is depicted. The plasma density is $\rho_0$ which was set according to the input current. An outer shell was given a density $A = 10$ times $\rho_0$ and was $\Delta R = 0.1$ cm thick. The initial radius was $R_0 = 2.0$ cm. The simulation was $L = 1.0$ cm wide with periodic boundary conditions.

The initial density profile is shown in Fig. 1. A deuterium shell with a radius of $R_0 = 2$ cm and a thickness of $\Delta R = 0.1$ cm enclosed a deuterium plasma with a density of $\rho_0$. The shell and inner plasma were assumed to be fully ionized. The density of the shell was $A = 10$ times the density of the fill. Values for $\Delta R$ and $A$ were chosen to be comparable to the dimensions of typical plasma sheaths observed in fully kinetic simulations of a DPF [16]. To keep a constant pinch time, the density for each current simulated was chosen to satisfy $I^2/\rho_0 = 3.05 \times 10^{-5}$ A$^2 \cdot$ cm$^3$. A parametric study at 1.5 MA was performed to select the values of $R_0$ and $\rho_0$ such that the neutron yield was optimized. To seed the RT instability, the density in the shell region was given a random speckle. Each cell was modulated by a uniform random value of ±6%. Hereafter, simulations with the 6% modulation are referred to as seeded simulations and those without are unseeded.

A hybrid fluid/kinetic model was used for 2-D simula-

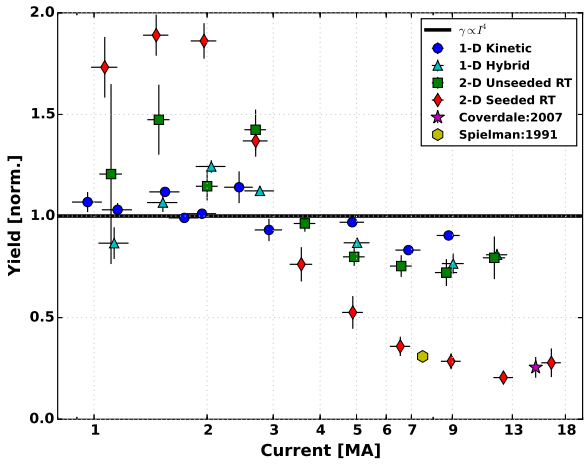


FIG. 2. (color online). Neutron yield normalized to the power law fit ($Y_n/L = 1.43 \times 10^9$ cm$^{-1} \cdot$ MA$^{-4} I^4$) of yield results from 1-D, kinetic simulations (blue dots) are plotted. Yields vary by an order of magnitude when a 6%, random density modulation was applied to seed RT instabilities (red diamonds). Experimental results from Spielman *et al.* [18] and Coverdale *et al.* [12] are shown for comparison.

tions. For the parameters used, the plasma pinch time was 46 ns. In the simulations, the first 42 ns of the plasma evolution were advanced using a quasi-neutral (QN), Eulerian fluid treatment. A description of the algorithm can be found in Thoma *et al.* [17]. After 42 ns, the QN treatment was no longer valid, and an automatic migration to a kinetic simulation occurred. The QN treatment was accurate for time steps that scale as $I^{-1}$. For 1 MA, the time step was $\Delta t = 3.3$ ps. In the kinetic phase, simulations require that the electron gyro-frequency be resolved ($\Delta t < 10 - 100$ fs) for stability. The kinetic phase of the simulations closely followed the fully kinetic simulations in Welch *et al.* [13], and specific details of the computational setup for this work are described therein. Use of the hybrid model substantially reduced the computational time required, enabling a thorough study to be performed.

Simulations were executed up to the point where the plasma reached its maximum excursion after the first pinch. Consistent with analytic scaling models [2, 3], neutrons produced in subsequent bounces after the first were not included in the tabulation. Neutron yields from the four different simulation series are presented in Fig. 2. The values have been normalized to a least-squares fit of the 1-D data, $Y_n/L = 1.43 \times 10^9$ cm$^{-1} \cdot$ MA$^{-4} I^4$. A distinct transition in neutron yield performance exists around 3 MA for all four series and is most significant in the case where RT was seeded. Error bars were computed by taking the size of the largest single fusion event and thus represent the macro particle nature of the fusion statistics.

The close agreement between 1-D hybrid simulations and 1-D fully kinetic simulations is validation for the accuracy of the hybrid model and the QN fluid to kinetic PIC migration algorithm. Plasma conditions such as density, temperature, and pinch radius at stagnation as well as and neutron yields were compared with experimental results and found to be similar as well. At stagnation, the pinch radii from the simulations were $\approx 3$ mm with ion temperatures between 4 to 6 keV, just as they were shown in Coverdale *et al.* [12]. Neutron yields at high currents also compare well with those published in Spielman *et al.* [18] and Coverdale *et al.* [12]. Furthermore, the neutron yields vs time were compared with the results shown in Welch *et al.* [3] and found to be in close agreement with data from Lsp and Mach2 simulations with regards to the pulse duration and amplitude.

Current dependent, non-Maxwellian features in the ion distributions in the 1-D runs and the unseeded 2-D runs can be explained by a mechanism identified in Thoma *et al.* [19]. At lower currents where the density is low and the collision frequency is negligible on the implosion time scale, beam-like deuterons are accelerated by a thin sheath field near the plasma-vacuum boundary via $\vec{J} \times \vec{B}$ which imparts additional energy to the ions as the sheath travels towards the axis. For seeded simulations, non-Maxwellian features are due to beam-like ions produced in the RT-induced electric fields.

Fig. 3 shows the electric field and the ion density, at stagnation, in the neighborhood of typical bubble and spike features from a seeded simulation at 8.9 MA. The E-field and density profile illustrate how beam-target fusion occurs. The direction of the electric field is roughly orthogonal to the narrow edge of high field regions. The magnitude of the field is between 200 and 1000 kV per mm, and the width of the feature is a fraction of a millimeter. In just a single interaction with this field, a deuteron could be accelerated to more than 200 keV in a direction roughly parallel to the z-axis. The presence of the strong magnetic field ($\approx 300$ T) directs the deuterons inward toward the cooler, denser fuel via the $\vec{E} \times \vec{B}$ drift.

The change in behavior around 3 MA is apparent in the energy distributions of the ions. In Fig. 4, the ion energy distribution, normalized to the peak value, for each current of the RT seeded simulations of deuterons inside a 2 mm radius are shown at the time of stagnation. For the first four currents below 3 MA, the distributions are nearly identical. After that, the high energy tail drops steadily, and the distribution approaches that of a Maxwellian with a temperature of 4.5 keV.

Before stagnation, the filaments seen in Fig. 3 are approximately 0.5 mm wide, oriented vertically, and have field vectors in the z-direction. The average magnitude of the E-field is proportional to the current, $\vec{E} = CI\hat{z}$, where $C$ is a constant of proportionality. Using the E-fields at the time of peak fluid velocity, 42 ns, a reasonable

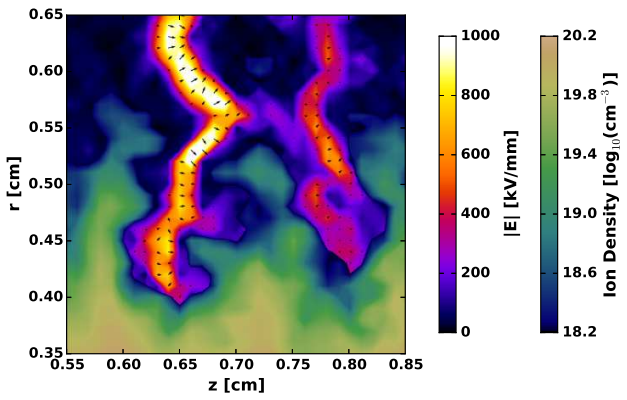


FIG. 3. (color online). Shown here are the electric field and ion density of a 8.9 MA, RT-seeded simulation at stagnation ($t =$ 46 ns). Field vector arrows are also shown.

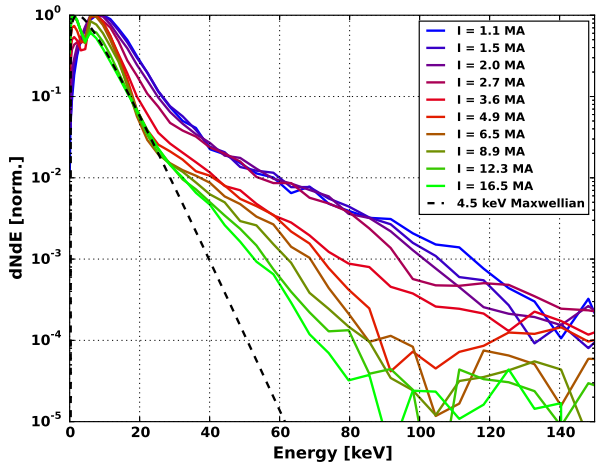


FIG. 4. (color online). The deuteron energy spectra of ions inside the pinch ($r < 2$ mm) for RT-seeded simulations at stagnation ($t =$ 46 ns), normalized to the peak value, for currents below 3 MA are virtually identical. Above 3 MA, the distributions converge to a thermal distribution with a temperature of 4.5 keV.

fit to the mean value of the high-field regions is given by $C = 26.3$ kV/mm$\cdot$MA. For the strongest fields, $C$ could be 5 to 10 times greater. Given that the B-field and the E-field are proportional to $I$, the current cancels when calculating the $\vec{E} \times \vec{B}$ drift velocity, and one gets,

$$v_{drift} = \frac{E}{B} = \frac{2\pi r C}{\mu_0}. \quad (1)$$

The gyrating particle motion along the z-axis has a corresponding amplitude given by,

$$r_{gyro} = \frac{m_D E}{eB^2} = \frac{4\pi^2 r^2 m_D C}{e\mu_0^2 I}, \quad (2)$$

where $m_D$ and $e$ are the mass and charge of a deuteron, respectively. For $r = 1.0$ cm, $r_{gyro} =$ 1.3 mm at 1 MA. The average kinetic energy of the deuterons accelerated by the E-field is $E_{drift} = {}^1/_2 m_D v_{drift}^2$. Again, using $r =$ 1.0 cm as a representative value, $E_{drift} =$ 18 keV. These numbers are only representative and do not account for time dependent variations of the electric field strength and the gradient in the magnetic field.

Beam ions whose velocities are greater than the implosion velocity can gain additional kinetic energy by way of Fermi acceleration [20, 21]. Once the ions have drifted into the core region of the plasma they will pick up additional energy with each reflection off the boundary of the incoming sheath. Assuming the sheath has an average velocity $u_{sheath}$, the deuteron velocity after the $n^{th}$ bounce is,

$$v_n = n u_{sheath} + v_{drift}. \quad (3)$$

The number of achievable bounces is limited by either the number of round trips though the plasma before stagnation ($n \approx v_n \tau / 2 r_{avg}$) or the distance traveled before being scattered ($n \approx \lambda / 2 r_{avg}$). Here, $r_{avg} \approx$ 1 cm is the average pinch radius during the lifetime of the beam particles, $\tau$ is approximately the pinch time, and $\lambda$ is a characteristic ion mean free path (mfp).

Ion-ion collisions limit the range for ions given the plasma conditions near stagnation. The mfp for a beam deuteron with a velocity, $v$, is computed as,

$$\lambda_{ii} = \frac{2\pi\epsilon_0^2 m_D^2 v^4}{e^4 n_D \ln\Lambda_{ii} \psi(x)}, \quad (4)$$

where $n_D$ is the deuteron number density, $\ln\Lambda_{ii}$ is the Coulomb logarithm, $x = m_D v^2 / 2kT_D$, and

$$\psi(x) = \frac{2}{\sqrt{\pi}} \int_0^x t^{1/2} e^{-t} dt. \quad (5)$$

The ion temperature is $T_D$.

For the simulations presented here, the pinch time $\tau$ is approximately 46 ns. Taking the average value of $E_{drift} =$ 18 keV, one might expect an increase in particle energy to 140 keV in the absence of collisions. This assumes $u_{sheath}$ is approximately equal to the maximum observed value of the average fluid velocity, $7.8 \times 10^5$ m/s, and the particles bounce an average of 3 times. This energy gain is consistent with the spectra for the lower currents shown in Fig. 4.

As long as $\lambda_{ii}$ is greater than the particle transit distance, the implosion time alone dictates how the accelerated ions impact the energy distribution. Since the implosion time is constant for every current, the ion distributions should be and are identical in this regime. For the aforementioned estimated value of the drift velocity, the total travel distance is about 6 cm. For an 18-keV deuteron, $\lambda_{ii}$ approaches this distance around 3 MA. The result is fewer transits and less energy gain from Fermi

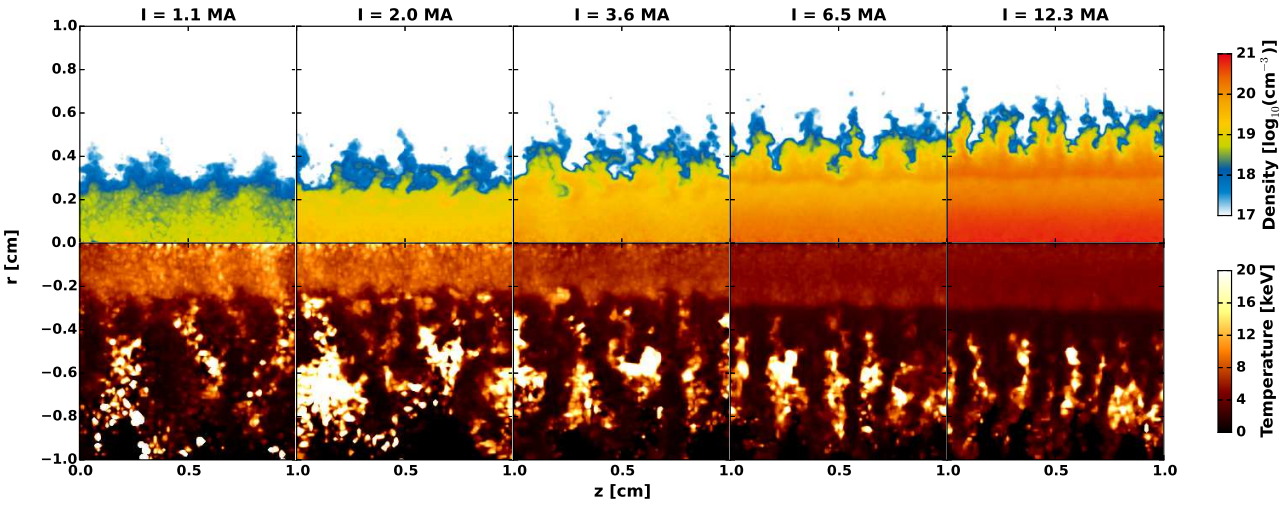


FIG. 5. (color online). The density (positive r-axis), and the temperature (negative r-axis) in the seeded simulations at stagnation show evidence of increased temperatures for the lower currents and decreased compression for larger currents. In the low currents, columns of high temperature are evident and are due to high energy deuterons injected by the $\vec{E} \times \vec{B}$ drift in the RT-induced fields. See Supplemental Material at [URL will be inserted by publisher] for an animated version of this figure.

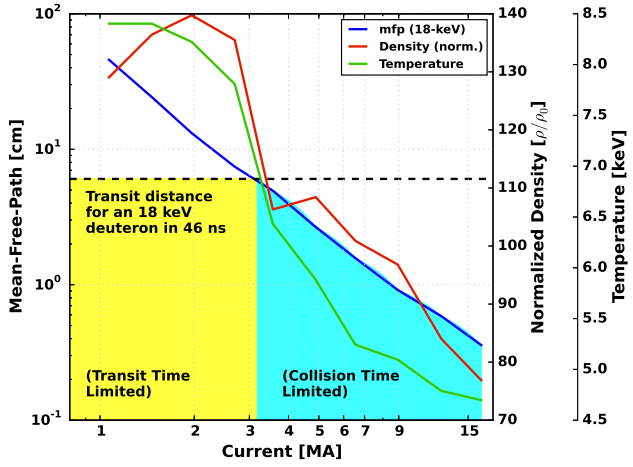


FIG. 6. (color online). Shown here is the ion mfp versus current for an 18-keV deuteron in the plasma core ($r < 2$ mm) at stagnation ($t =$ 46 ns) for seeded simulations. Also shown are the core density and temperature.

acceleration. At the highest currents simulated, $\lambda_{ii}$ is on the order of a few millimeters. In this regime, beam ions are unable to penetrate the dense core. Beam-target fusion is restricted to interactions with the RT spikes and beam ions cannot assume energy from the inbound sheath via Fermi acceleration.

From a qualitative look at Fig. 5, it is clear to see that for the lower currents, higher temperatures do exist in the compressed core of the pinch. In the absence of beam deuterons, the temperature should remain constant for every current. Furthermore, the increased temperatures in the low current simulations have structures which connect seamlessly with the high energy particles produced in the RT induced electric fields. The behavior changes above 3 MA. Four observations stand out. First, the temperature in the core regions are cooler and uniform. Second, the hot structures outside the core region are fully disconnected from the dense core. Third, the radius of the compressed region is slightly larger for higher currents than it is for lower currents. Fourth, a high density boundary has formed, separating the RT spikes from the inner core plasma. This dense layer has formed as a result of snowplowing ions due to the millimeter scale $\lambda_{ii}$.

Fig. 6 shows $\lambda_{ii}$ of an 18-keV deuteron through the dense core ($r < 2$ mm) of the plasma at the time of stagnation for each current for RT-seeded simulations. Also shown are the density and temperature of the core. As observed in Fig. 5, $\lambda_{ii}$ for the average $\vec{E} \times \vec{B}$ drifting deuteron is too short for significant penetration into the core region at high currents.

For the identical, non-Maxwellian spectra enhanced in the transit-time-limited regime ($I < 3$ MA), the neutron yield varies as $n_D^2 \propto I^4$. In the collision-time-limited regime, the neutron yield decreases as decreasing values of $\lambda_{ii}$ effectively disable the enhancement. For currents great enough, neutrons are produced predominantly from thermonuclear fusion, which also scales as $I^4$. Without the RT-produced enhancement benefited by low currents and diminished thermonuclear performance due to RT, scaling drops by nearly a factor of 10 in the high current regime relative to the low-current regime.

In summary, observations of a direct mechanism which contributes to the dramatic drop in fusion yield scaling for currents above a few MA have been presented. Understanding the shift in yield has been a standing problem for nearly 50 years with only speculative solutions given [4]. The simulations show that for a constant pinch time with a constant initial radius, low-current pinches experience an enhancement in fusion yield because of high energy, beam-like particles accelerated by RT-induced fields. For higher currents, however, the increased stopping power of the plasma prevents the beam-like particles from participating. While this work does not show the factor of 100 presented in Krishnann *et al.* [4], it should be noted that the simulations in this work do not address the influences of contaminants from electrode surfaces nor the role of azimuthal variations of RT structures one observes in 3-D simulations [22–24]. Incorporation of these important elements is required to achieve a more quantitative agreement and will be the topic of future work.

The authors would like to acknowledge Dr. Radu Presura and Peggy Voss of Voss Scientific for their comments. Thanks are also given to Dr. Nicki Bennett of National Security Technologies (NSTec) for her review. This research was developed with funding from the Defense Advanced Research Projects Agency (DARPA). The views, opinions, and/or findings contained in this article are those of the authors and should not be interpreted as representing the official views or policies of the Department of Defense or the U.S. Government. *(Approved for Public Release, Distribution Unlimited.)*

* dustino@vosssci.com

[1] A. Bernard, P. Cloth, H. Conrads, A. Coudeville, G. Gourlan, A. Jolas, C. Maisonnier, and J. Rager, Nuclear Instruments and Methods **145**, 191 (1977).

[2] A. L. Velikovich, R. W. Clark, J. Davis, Y. K. Chong, C. Deeney, C. A. Coverdale, C. L. Ruiz, G. W. Cooper, A. J. Nelson, J. Franklin, and L. I. Rudakov, Phys. Plasmas **14**, 022701 (2007).

[3] D. R. Welch, D. V. Rose, C. Thoma, R. E. Clark, C. B. Mostrom, W. A. Stygar, and R. J. Leeper, Phys. Plasmas **17**, 072702 (2010).

[4] M. Krishnan, Plasma Science, IEEE Transactions on **40**, 3189 (2012).

[5] R. Verma, R. Rawat, P. Lee, M. Krishnan, S. Springham, and T. Tan, Plasma Science, IEEE Transactions on **38**, 652 (2010).

[6] V. I. Krauz, Plasma Physics and Controlled Fusion **48**, B221 (2006).

[7] J. De Groot and T. Mehlhorn, in *Plasma Science, 2004. ICOPS 2004. IEEE Conference Record - Abstracts. The 31st IEEE International Conference on* (2004) pp. 203–.

[8] C. Hartman, G. Carlson, M. Hoffman, R. Werner, and D. Cheng, Nucl. Fusion **17**, 909 (1977).

[9] H. Herold, A. Jerzykiewicz, M. Sadowski, and H. Schmidt, Nucl. Fusion **29**, 1255 (1989).

[10] E. J. Lerner and H. R. Yousefi, Phys. Plasmas **21**, 102706 (2014).

[11] D. Klir, J. Kravarik, P. Kubes, K. Rezac, S. Ananev, Y. Bakshaev, P. I. Blinov, A. Chernenko, E. Kazakov, V. D. Korolev, G. Ustroev, L. Juha, J. Krasa, and A. Velyhan, Plasma Science, IEEE Transactions on **37**, 425 (2009).

[12] C. A. Coverdale, C. Deeney, A. L. Velikovich, J. Davis, R. W. Clark, Y. K. Chong, J. Chittenden, S. Chantrenne, C. L. Ruiz, G. W. Cooper, A. J. Nelson, J. Franklin, P. D. LePell, J. P. Apruzese, J. Levine, and J. Banister, Phys. Plasmas **14**, 056309 (2007).

[13] D. R. Welch, D. V. Rose, R. E. Clark, C. B. Mostrom, W. A. Stygar, and R. J. Leeper, Phys. Rev. Lett. **103**, 255002 (2009).

[14] Lsp is a software product of ATK Mission Research, Albuquerque, NM 87110.

[15] T. P. Hughes, R. E. Clark, and S. S. Yu, Phys. Rev. ST Accel. Beams **2**, 110401 (1999).

[16] A. Schmidt, V. Tang, and D. Welch, Phys. Rev. Lett. **109**, 205003 (2012).

[17] C. Thoma, D. R. Welch, R. E. Clark, N. Bruner, J. J. MacFarlane, and I. E. Golovkin, Phys. Plasmas **18**, 103507 (2011).

[18] R. B. Spielman, G. T. Baldwin, R. J. Leeper, C. L. Ruiz, and G. Cooper, in *Plasma Science, 1991. IEEE Conference Record - Abstracts., 1991 IEEE International Conference on* (1991) pp. 203–204.

[19] C. Thoma, D. R. Welch, and T. P. Hughes, Phys. Plasmas **16**, 032103 (2009).

[20] R. Deutsch and W. Kies, Plasma Physics and Controlled Fusion **30**, 263 (1988).

[21] E. Fermi, Phys. Rev. **75**, 1169 (1949).

[22] E. P. Yu, A. L. Velikovich, and Y. Maron, Phys. Plasmas **21**, 082703 (2014), http://dx.doi.org/10.1063/1.4891844.

[23] E. P. Yu, M. E. Cuneo, M. P. Desjarlais, R. W. Lemke, D. B. Sinars, T. A. Haill, E. M. Waisman, G. R. Bennett, C. A. Jennings, T. A. Mehlhorn, T. A. Brunner, H. L. Hanshaw, J. L. Porter, W. A. Stygar, and L. I. Rudakov, Phys. Plasmas **15**, 056301 (2008), http://dx.doi.org/10.1063/1.2837050.

[24] P. Kubes, M. Paduch, J. Cikhardt, J. Kortanek, B. Cikhardtova, K. Rezac, D. Klir, J. Kravarik, and E. Zielinska, Phys. Plasmas **21**, 122706 (2014), http://dx.doi.org/10.1063/1.4903906.